5 Analytical Model

5.1 OVERVIEW

The field of fracture mechanics originated in the early 1950's in the form of analytical solutions. Many of the concepts have been discussed in Chapter 2, and these concepts generally can be applied with little modification to predict crack behavior in virtually any scenario involving elastic materials. The stress intensity factor, or K, serves as the principle parameter for determining the crack driving force. For fatigue crack growth, the stress intensity factor range is used to evaluate the propagation rate through the Paris Law, repeated here for convenience:

$$\frac{da}{dN} = C(\Delta K)^m$$

A center-cracked panel has long served as a basis for demonstrating the principles of fracture mechanics. In fact, the stress intensity factor for many different cracking situations has been related to the center-cracked tension (CCT) K solution through magnifying coefficients. Cracks in stiffened panels take on this form directly, where the resulting K for a stiffened panel is expressed as a ratio to the unstiffened panel K. This normalization provides an easy means for characterizing the relative severity of a crack scenario.

The analytical model used in this research superimposes K solutions that have been previously developed and are readily available in handbooks. The model was first developed on this basic principle of superposition and then compared with the finite element model, discussed in the following chapter. The results and corresponding modifications will also be discussed in Chapter 7. Chapter two introduced the work of Poe that had been recently used by Nussbaumer in box girder crack prediction. This model serves as the basis for the current model development. Superimposing the effects of stiffener restraint, stiffener separation, and residual stress is the basic procedure that will be defined in this chapter. An overview of the superposition is presented in Figure 5-1.

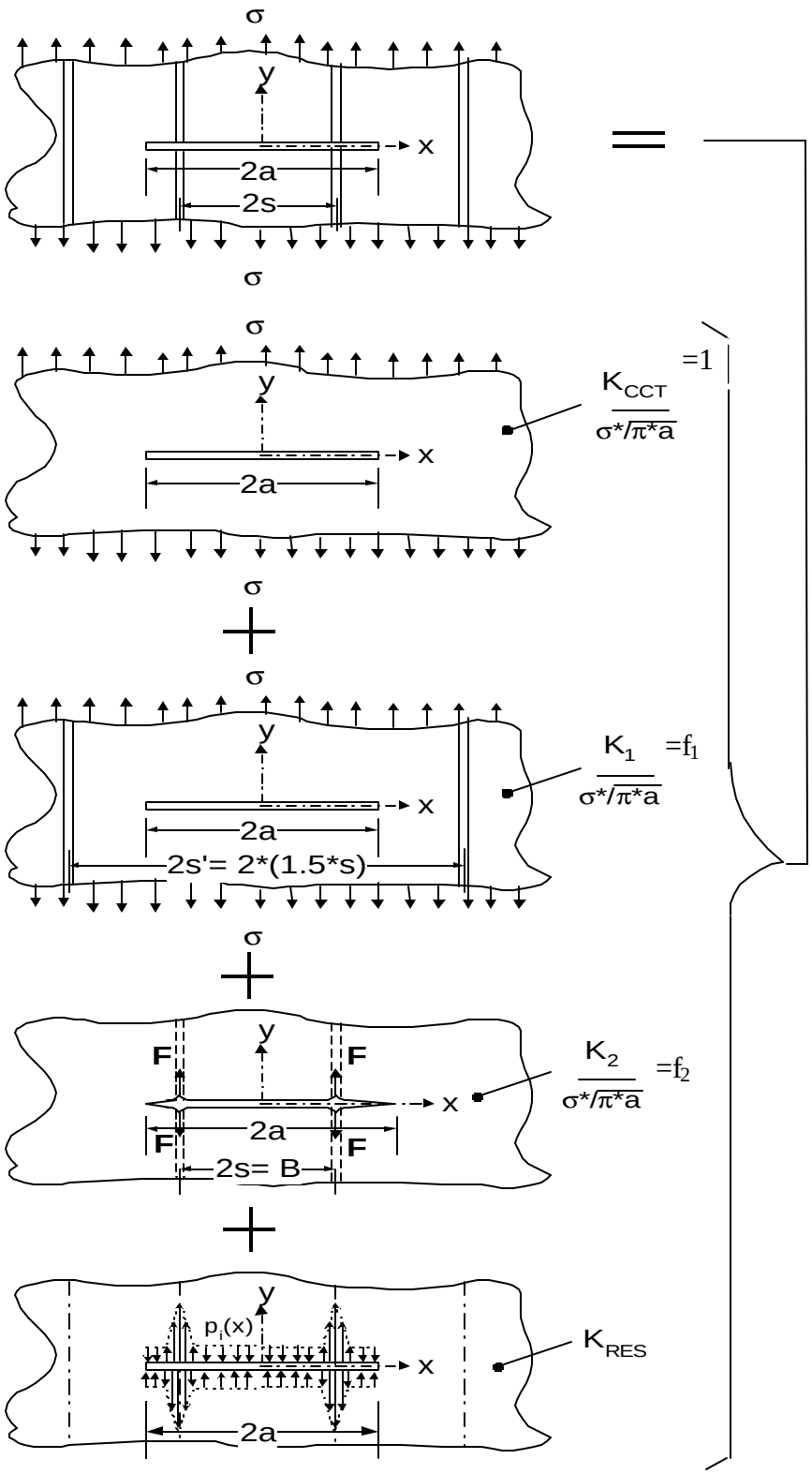

Figure 5-1: Overview of superposition components.

The experimental investigation focused on a case study that would be relatively easy to analyze in order to verify the models. That is, the condition of a crack centrally located between two stiffeners, although unrealistic, provides a valuable basis for model development. The following analytical solutions are developed specifically for a centrally located crack in a stiffened panel. Cracks that are centered about a stiffener would have slightly different K-formulations. Nonetheless, the following analytical model will soundly define the procedure for analysis.

5.2 EFFECT OF STIFFENER RESTRAINT

The first effect that modifies the CCT K is that of stiffener restraint. In Figure 5-1, this effect is represented by f_1. Isida [76] originally developed the stress intensity factor for a sheet with stiffened edges. Nussbaumer manipulated his solution into a form that would be suitable for panels with multiple, continuously attached stiffeners. He modified Isida's work by assuming negligible bending stiffness in the stiffeners and removing the built-in correction for finite width. A brief summary of Nussbaumer's derivation will be provided here.

Isida's stress intensity factor for the finite width sheet with stiffened edges utilized two parameters: β and χ. The first parameter, β, represents the axial stiffness of the stiffeners relative to the area of the plate it is responsible for stiffening, or its tributary plate area. Written expressly:

$$b = \frac{A_{st}}{t_{pl} s} \qquad \text{Eqn. 5-1}$$

where s is half the stiffener spacing and t_{pl} is the plate thickness. The formulation for χ is just the normalized crack distance:

$$c = \frac{a}{s} \qquad \text{Eqn. 5-2}$$

where a is half the crack's total length. Isida's solution is accurate for all values of χ less than 0.95. Nussbaumer examined Isida's Fourier series solution for three values of β: 0, 1 and infinity. β-values between one and infinity could be represented adequately by using an abbreviation of Isida's formulation:

$$f_{Isida} = (f_k - 1)\left(\frac{1}{1+b}\right)^{a_1} + 1 + 0.3c^2\left(\frac{4}{b^2 - 2b + 4} - 1\right) - a_2\left(c^{10} + c^{30} + c^{50}\right)\left(\frac{4}{b^2 - 2b + 4} + 1\right)$$

Eqn. 5-3

where α_1 and α_2 characterize the magnitude of the edge stiffener's restraint. Also in the equation is the dimensionless variable f_k known as Koiter's finite width correction. The finite width correction accounts for increased net section stresses, and corresponding higher K values, as a crack grows in a plate of finite size. Koiter's correction is defined as follows:

$$f_k = \frac{1 - 0.5c + 0.326c^2}{\sqrt{1 - c}} \qquad \text{Eqn. 5-4}$$

Koiter's solution is a finite width correction factor that is accurate to 1 percent over a wide range of χ. When β is zero, f_{Isida} defaults to Koiter's solution, appropriately so since a β of zero corresponds to an unstiffened plate.

With non-zero β, f_{Isida} provides a reduction factor to account for stiffeners at $\chi = 1$. To obtain the solution for an *infinite plate* with a pair of stiffeners, one merely divides Isida's coefficient by the finite width correction factor. The infinite plate result is as follows:

$$f_1 = \left(1 - \frac{1}{f_k}\right)\left(\frac{1}{1+b}\right)^{a_1} + \frac{1}{f_k} + \frac{0.3c^2}{f_k}\left(\frac{4}{b^2 - 2b + 4} - 1\right) - a_2\left(\frac{c^{10} + c^{30} + c^{50}}{f_k}\right)\left(\frac{4}{b^2 - 2b + 4} + 1\right) \quad \text{for } c \le 0.95 \qquad \text{Eqn. 5-5}$$

There are a few components that one may take notice of in this equation. First of all, the term $1/f_k$ corresponds to an infinite unstiffened plate. To isolate the reduction in stress intensity factor due to the edge stiffeners, merely subtract one from the above formulation. Secondly, the effect of multiple stiffeners may be addressed by determining $f_{1,i}$ for each i^{th}

pair of stiffeners at a distance χ_i from the center of the panel. This approach overestimates the restraining effects of the stiffeners. Therefore, Nussbaumer calibrated the formulation to fit Poe's results by setting $\alpha_1 = 1$ and $\alpha_2 = 0.1$. These parameters are calibration constants that should be applicable to most stiffened panel configurations. Refinement of α_1 and α_2 may be performed for unusual stiffening elements through comparison with equivalent K-solutions determined from finite element analysis. However, for stiffened panels in use today the determined values are suitable. The restraint contribution of a pair of stiffeners at a distance χ_i may be determined by the following equation:

$$f_1 = \left(1 - \frac{1}{f_{k,i}}\left(\frac{1}{1+b_i}\right)^{a_1} + \frac{1}{f_{k,i}} + \frac{0.3c_i^{\,2}}{f_{k,i}}\left(\frac{4}{b_i^{\,2} - 2b_i + 4} - 1\right)\right) - 1$$
$$- a_2\left(\frac{c_i^{\,10} + c_i^{\,30} + c_i^{\,50}}{f_{k,i}}\right)\left(\frac{4}{b_i^{\,2} - 2b_i + 4} + 1\right) \qquad \text{for } c \le 0.95 \qquad \text{Eqn. 5-6}$$

where $c_i = \frac{a}{x_i}$ and $b_i = \frac{A_{st,i}}{t_{pl} x_i}$. Here x_i is the distance to the i^{th} stiffener and $A_{st,i}$ is its respective area.

The final coefficient may be found by summing the restraint effects for each set of intact stiffeners:

$$f_1 = \sum f_{1,i} \qquad \text{Eqn. 5-7}$$

It is important to note that the effect of stiffener restraint, from this point forward referred to as the "first effect", is only accurate for χ_i less than 0.95. For panels with multiple stiffeners, this limitation becomes evident as a crack is grown across many stiffener spans. Furthermore, this limitation does not allow the crack to grow near or into a stiffener. Therefore, interpolation must be used between a crack of length $\chi_i = 0.95$, using the f_1 coefficient, and a crack that has grown past the stiffener, using the f_2 coefficient. The f_2 coefficient is discussed in the next section.

5.3 EFFECT OF SEVERED STIFFENERS

The second effect to be accounted for is the effect of severed stiffeners. This effect is addressed by a second correction factor termed f_2. Severed stiffeners are treated as point forces applied to the crack face, as shown in Figure 5-2.

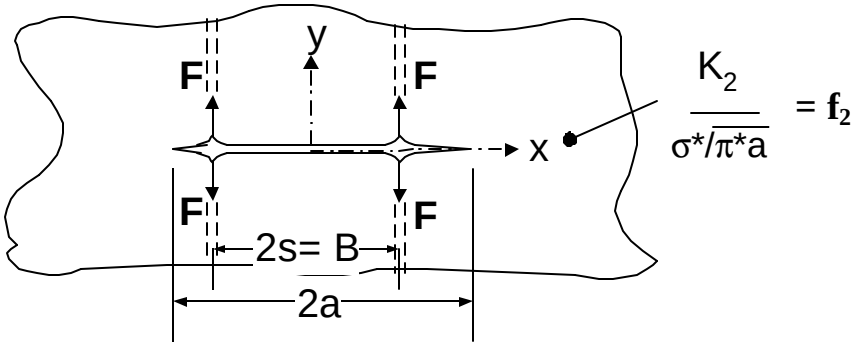

Figure 5-2: Severed stiffeners treated as point forces.

The magnitude of the point force is simply the force that was formerly carried by the intact stiffener,

$$F = sA_{st,i} = s\left(\frac{m}{m-1}\right)\left(A_{pl}\right) \qquad \text{Eqn. 5-8}$$

where $m = \dfrac{A_{st}}{A_{st} + A_{pl}}$, and $A_{pl} = 2st_{pl}$ for the crack configuration under investigation. The stress intensity factor is represented as a pair of splitting forces acting on the crack face. Its formulation is readily found in stress intensity factor handbooks as:

$$K = \frac{2F}{t_{pl}\sqrt{pa}}\frac{a}{\sqrt{a^2 - s^2}} \qquad \text{Eqn. 5-9}$$

As in the formulation of the first effect, the second effect may be transformed to a magnification of the unstiffened plate K with the same crack length. This transformation

turns the above stress intensity factor into the correction factor f_2. Further algebraic manipulation of the equation allows the use of common parameters χ_i and μ:

$$f_{2,i} = \frac{2m}{p(1-m)} \frac{2s/x_i}{\sqrt{c_i^{\,2} - 1}} \quad \text{for } \chi_i > 1 \qquad \text{Eqn. 5-10}$$

where x_i is the actual distance to the i^{th} severed stiffener and χ_i is the normalized distance to the i^{th} severed stiffener. The above equation is used for each pair of severed stiffeners and summed to give the total f_2 coefficient.

5.4 ASSEMBLY OF STIFFENED PANEL COEFFICIENT

Now that the first and second effects have been formulated, one may assemble the coefficients to obtain the complete coefficient for an individual crack length. The assembly may be expressed as:

$$f_{st} = 1 + \sum f_{1,i} + \sum f_{2,i} \qquad \text{Eqn. 5-11}$$

where one represents the unstiffened plate. Figure 5-3 shows the assembled coefficient and the relative contributions of the first and second effects.

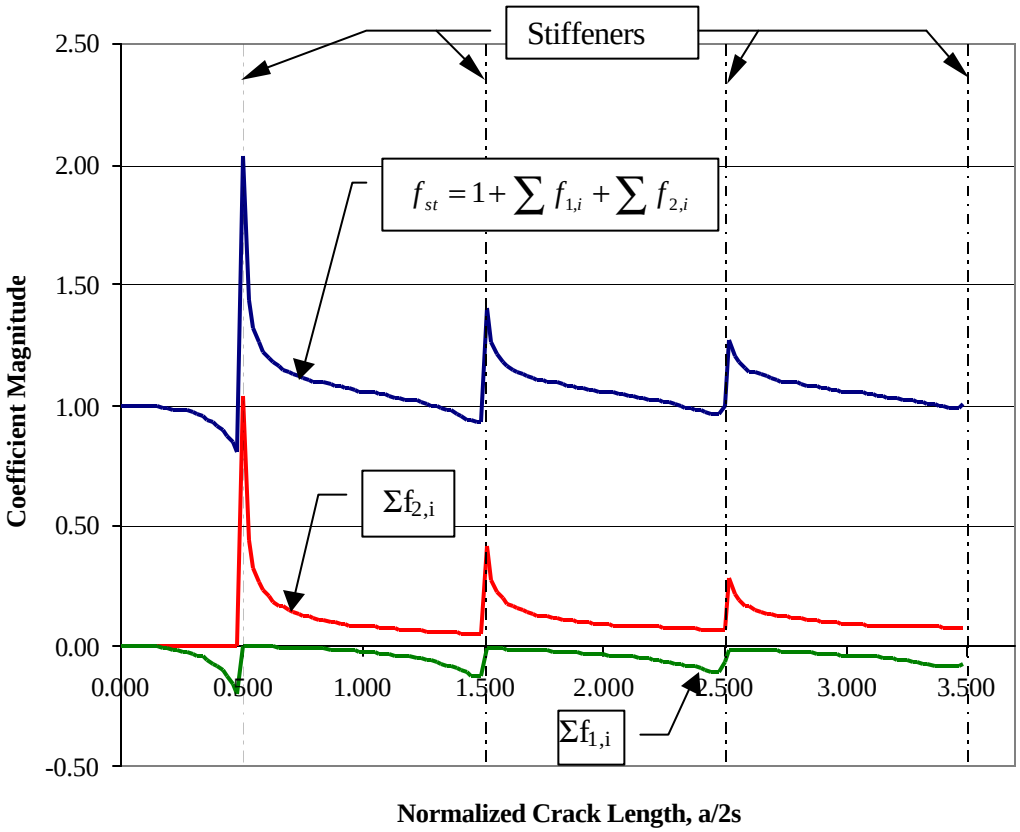

Figure 5-3: Assembly of stiffened panel correction coefficient.

One may observe the sharp discontinuity that forms as a crack approaches the stiffener. The discontinuity results from the assumption that the stiffener is severed immediately once the crack reaches it. In reality, the stiffener crack growth has been observed to match the growth in the plate. Using this observation, one may use linear interpolation between the coefficient for an unsevered stiffener and a severed stiffener.

Another observation is the general decrease in the effect of severed stiffeners as the crack surpasses several stiffener spans. This may be explained by the normalization of the plot. The coefficient is given as a ratio to the unstiffened panel K solution, and at large crack lengths the magnitude of the K-factor becomes significant enough that contributions from additional severed stiffeners increases the corresponding K-factor only marginally. In other

words, a point force on a large crack will generate less of an impact on the total K-factor than the same magnitude point force acting on a small crack.

The first point of interpolation is defined as the last accurate correction coefficient prior to a crack surpassing a stiffener, namely χ_i= 0.95. One may find the second interpolation point by assuming a radius equal to the distance of the plate crack from the stiffener centerline. Poe originally developed this procedure, which may be seen graphically in Figure 5-4.

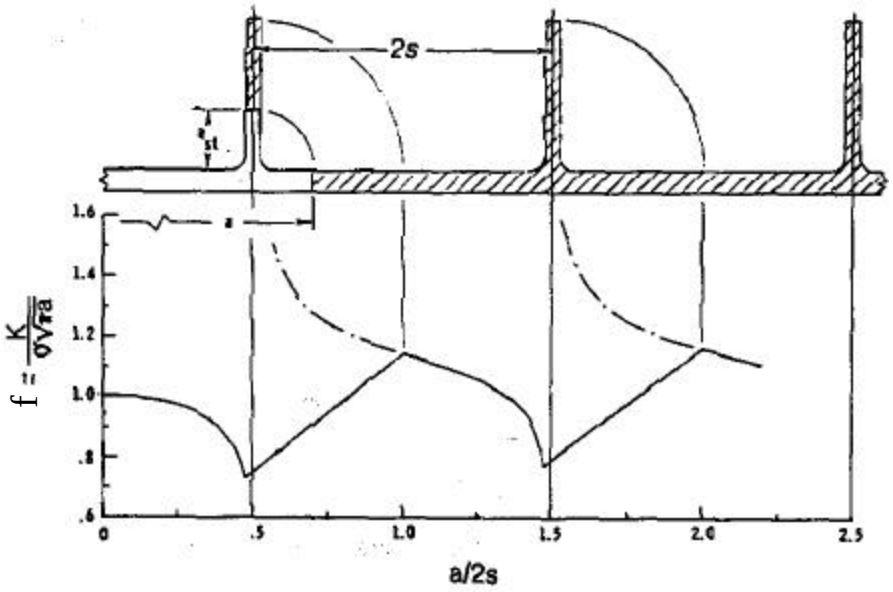

Figure 5-4: Interpolation between unbroken and broken stiffeners [Poe, 66].

Using this procedure, a comparison may be made between various stiffness ratios. Figure 5-5 shows the effect of changing the stiffness ratio.

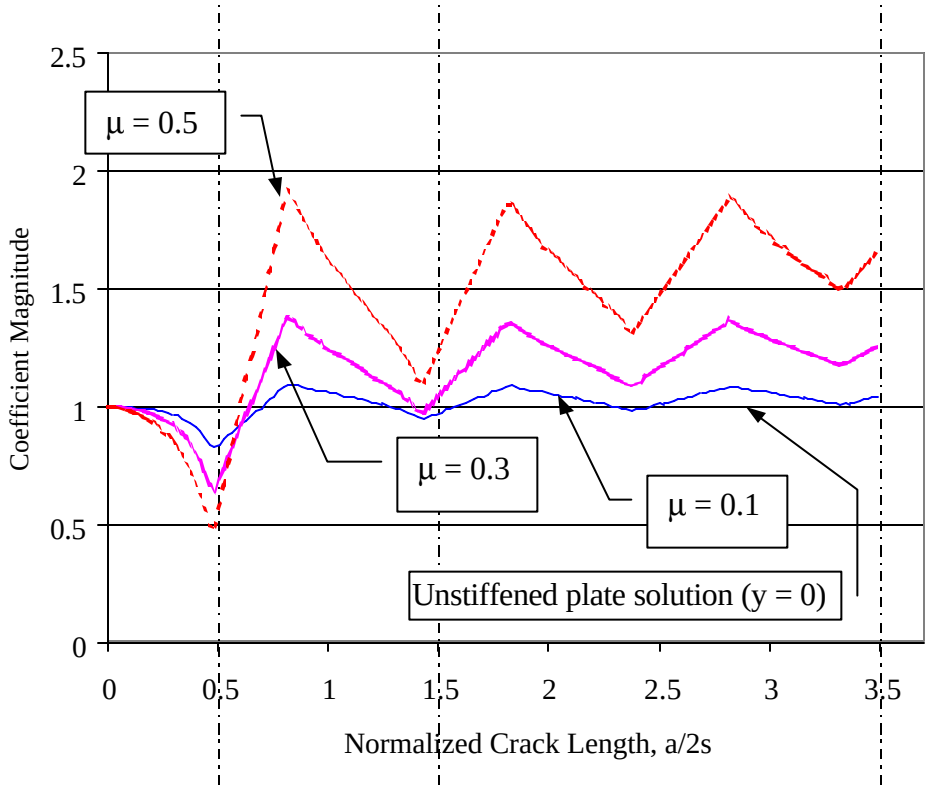

Figure 5-5: Effect of changing stiffness ratio on correction factor.

As the stiffness ratio increases, the curves for f_1 and f_2 diverge. Nussbaumer found that stiffness ratios less than 0.7 result in behavior resembling that of Poe's work. He noted that, in typical cellular structure, stiffness ratios are less than 0.5 and thus the model is applicable. In the experimental scope of this research the stiffness ratios were held constant at μ=0.22.

The stiffened panel stress intensity factor has so far been illustrated without correcting for the effects of finite width. Many functions exist to make this correction, including the net section change coefficient presented by Nussbaumer. This compliance coefficient, which is Equation 2-17, is repeated here for convenience:

$$f_s = \frac{s}{s_{nom}} = \frac{I_0 c(a)}{I(a) c_0} \qquad \text{Eqn. 5-12}$$

This correction factor is used as a multiplier to the total stress intensity factor. It provides an easy means of relating the increase in applied stresses to crack growth. The final result for the stiffened panel stress intensity factor is expressed as follows:

$$K_{st}(a, f_1, f_2) = f_s \left(1 + \sum f_{1,i} + \sum f_{2,i}\right)\left(s\sqrt{pa}\right) = f_s\, f_{st}\, s\sqrt{pa} \qquad \text{Eqn. 5-13}$$

5.5 RESIDUAL STRESS INTENSITY FACTOR

Residual stress effects on crack growth are taken into consideration separately from the previous components. This is because the applied stresses are assumed to not affect the magnitude of the residual stress distribution. A stress intensity factor is developed to account for its presence assuming no redistribution during cracking. After the residual stress intensity factor is determined, it is added to the applied stress intensity factor as explained in Figure 2-5.

The analytical model presented uses the same residual stress intensity factor as utilized by Nussbaumer [109] and Thayamballi [154]. Its formulation has been previously shown in Figure 2-10 but will be repeated here for convenience:

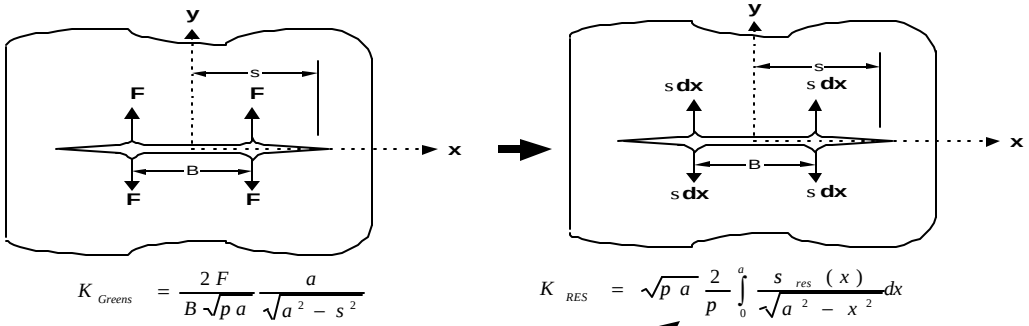

Figure 5-6: Development of residual stress intensity factor.

The residual stress intensity factor requires that the residual stress distribution be defined. In this analytical model, Faulkner's recommendations will be utilized. Faulkner's characterization of residual stress has been previously discussed in Section 3.5. The relatively simple model is practical in light of the scatter in residual stress data both in the laboratory and in actual ship measurements [114].

The residual stress distribution used in most of the analytical analyses is shown in Figure 5-7. For comparison, the measured data is presented also. The triangular tensile region has a base width of 3.5 times the plate thickness on either side of a stiffener. The peak of the tensile stress is the material yield stress. In determining the residual stress field, residual stress contributions from the stiffeners were neglected. This methodology provides an extremely simple means to develop the residual stress field for use in the residual stress intensity factor.

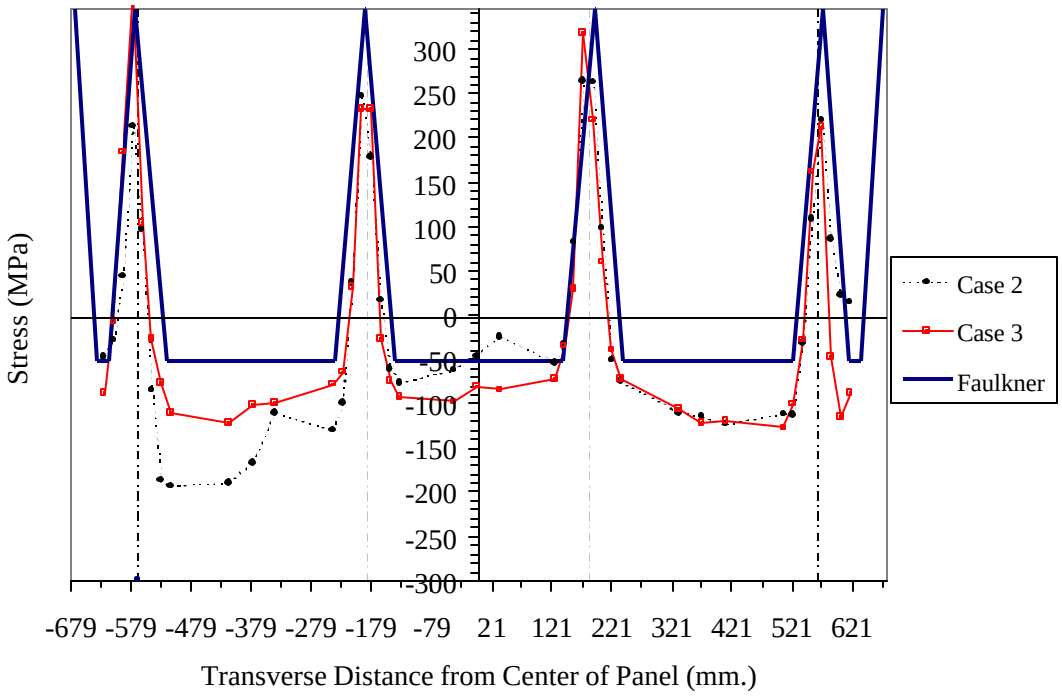

Figure 5-7: Faulkner residual stress model compared to measured values.

It is important to realize that the only effect residual stress has on the proposed models is to reduce the growth rate in regions of high compressive stress. In regions of tensile stress, the residual stress poses no impact on the analysis prediction since crack growth is a function of the effective stress *range*. That is, for positive residual stress intensity factors, crack growth is affected only by the applied stress range regardless of the magnitude of the residual stress intensity factor.

This behavior is explained in the concept of crack closure: Only the portion of the applied stress range in which the crack is open contributes toward crack growth. If compressive stresses hold the crack closed for a portion of the applied stress range, that portion is considered ineffective.

First, these calculations are for the case where the applied stress range is entirely in tension, i.e. that the minimum applied stress is equal to zero. While the typical wave-induced stress range is fully reversed, i.e. equal parts tension and compression with a mean stress of zero, there are situations where there is a tensile mean stress. For example, secondary or tertiary loading, such as the loading from water pressure, may put the structure locally into tension. A minimum applied stress of zero is typically a conservative assumption but it can be revised if better information is available. Situations where the stress range is partially in compression can be modeled in the same way simply by truncating the part of the applied stress range that is in compression. There are some cases of very high tensile mean stress where the minimum stress would be much greater than zero and this assumption could be unconservative. However, these cases are considered rare.

A crack growing in a residual-stress-free plate with a minimum applied stress of zero actually has some crack closure. Previous research [36] shows that the crack does not open until about 20 percent of the applied stress range under these conditions. This crack closure is also ignored in the model, making it more conservative since the crack closure is beneficial and tends to reduce crack growth rate. Therefore, this case without residual stress

represents the worst possible conditions, the crack is fully open during the entire stress range. Additional tensile residual stress cannot make things worse.

An evaluation of the residual stress intensity factor may be seen in Figure 5-8.

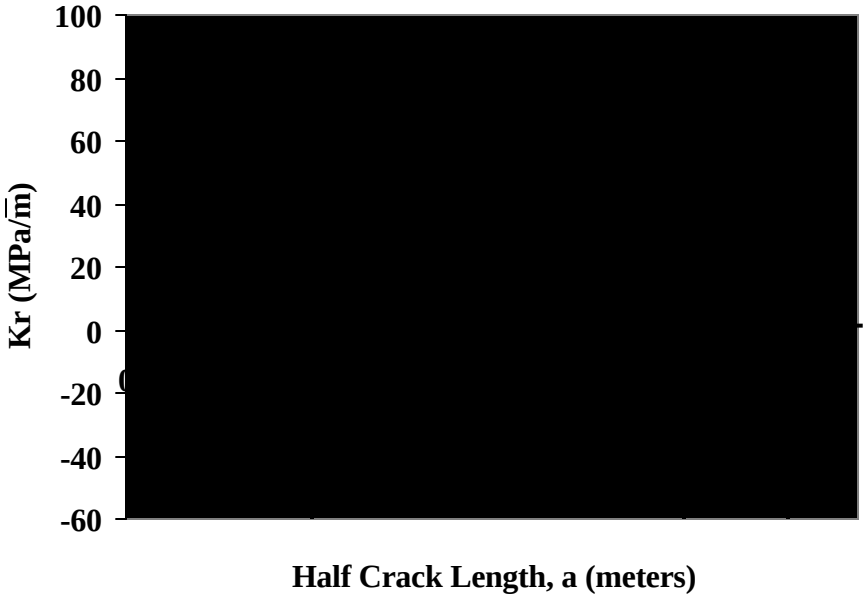

Figure 5-8: Resulting residual stress intensity factor for typical specimen.

5.6 PLASTICITY EFFECTS

Plasticity effects become important as applied stresses increase. In the course of this research, however, the effects of plasticity have been ignored. Justification lies in the low stress ranges used in the experiments, where plasticity effects are deemed negligible and are set to zero. This justification extends to the use of the models for evaluation of fatigue cracking in ship structure because most of the life of the ship undergoes stress ranges well below the yield strength of the material.

Nussbaumer [109] discredited the inclusion of plasticity effects in his models as well. He cited similar reasoning while also noticing that the effects of local plastic strain reversal tend

to propagate cracks "in a manner proportional to $(\Delta K)^m$." For these reasons, $K_{pl} = 0$ in the models proposed and analyses made.

5.7 SUPERPOSITION OF ANALYTICAL MODEL COMPONENTS

In this section a procedure will be reviewed to obtain the effective stress intensity factor range, the key parameter used in fatigue life prediction. The effective stress intensity factor is directly used in the Paris Law to predict the number of cycles for an incremental growth, *da*. Solving Equation 2-4 for the number of cycles yields:

$$dN = \frac{da}{C\left(\Delta K_{eff}\right)^m}$$

where $C = 9.5 \times 10^{-12}$ and m =3 for steel. There is some debate over the values to be used for C (Discussed in more detail in Chapter 2), but the author has chosen these values for upper bounds in connection with BSI PD6493 [23].

Figure 2-5, repeated here for convenience, provides the most straightforward instruction for determining the effective stress intensity factor. Recall that $K_{pl} = 0$ in the models proposed.

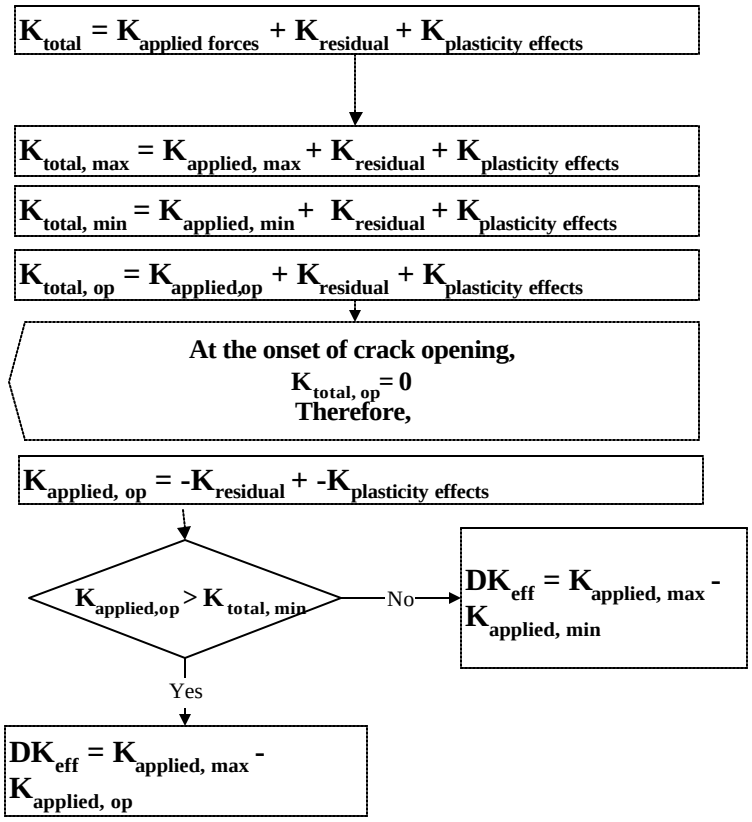

Figure 5-9: Procedure for determining stress intensity actor range.

In essence, one determines the stress intensity factor for both the minimum and maximum applied stresses. These quantities are appropriately termed the applied stress intensity factors. For example, the maximum applied stress intensity factor would be:

$$K_{app,\max} = f_s \, f_{st} s_{\max} \sqrt{pa} \qquad \text{Eqn. 5-14}$$

Next, one adds the residual stress intensity factor, a constant, to both of the applied stress intensity factors. The quantities are now called the total stress intensity factors. If neither of the total stress intensity factors is positive, it indicates that the crack is not opening even under the maximum applied stress. The effective stress intensity factor would be zero, then, and crack growth could not occur.

If the only the maximum total stress intensity factor is positive, it indicates that only part of the applied stress range is effective. Finally, the whole stress range is effective if both maximum and minimum total stress intensity factors are positive. A plot of an analytical model analysis can be seen in Figure 5-10.

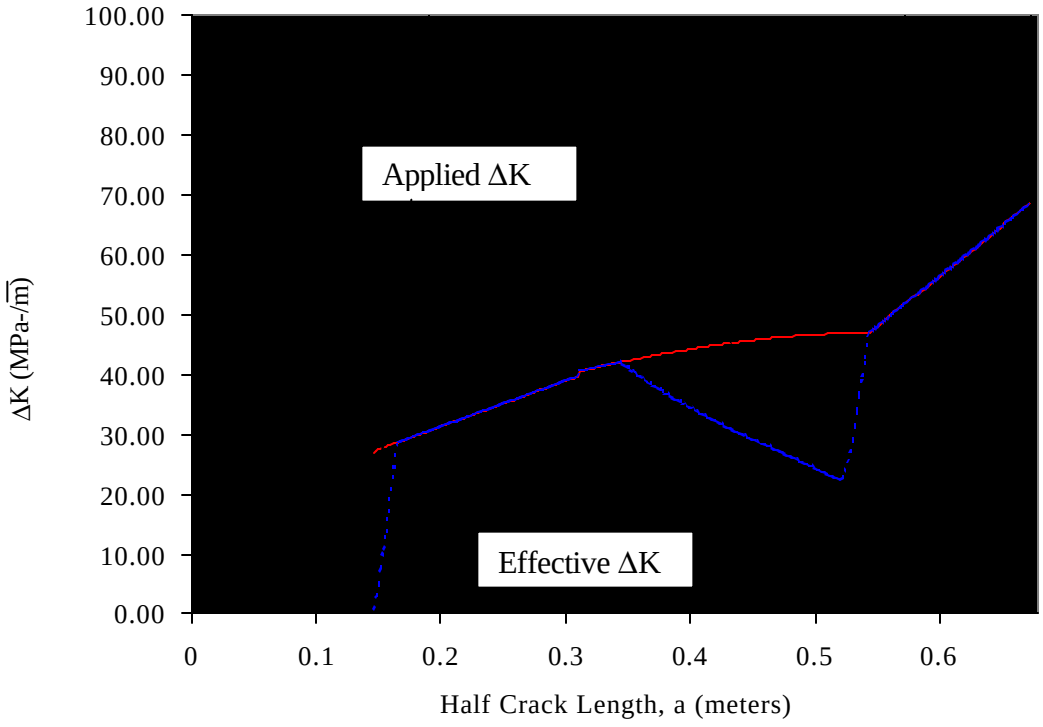

Figure 5-10: Difference between ΔK_{app} and ΔK_{eff} for stiffened panel

with σ_{max}=46 MPa and σ_{min}=6 MPa.

The effective stress range is defined as Elber's ratio, U, defined in Equation 2-8. Plotting Elber's ratio allows one to observe the residual stress influence on the effective stress intensity factor. Since the residual stresses are treated as constants, they do not promote increased fatigue crack growth in these models for any given crack length.

The region before the crack meets the first stiffener is highly sensitive to the compressive residual stress. In fact, for half crack lengths less than 146 mm no propagation would occur, as illustrated by Figure 5-11. Notice the rise in Elber's ratio between a = 0.145 meters and a = 0.175 meters. For cracks starting in a compressive residual stress region, this steep rise is an indicator that several analyses with different starting lengths should be performed.

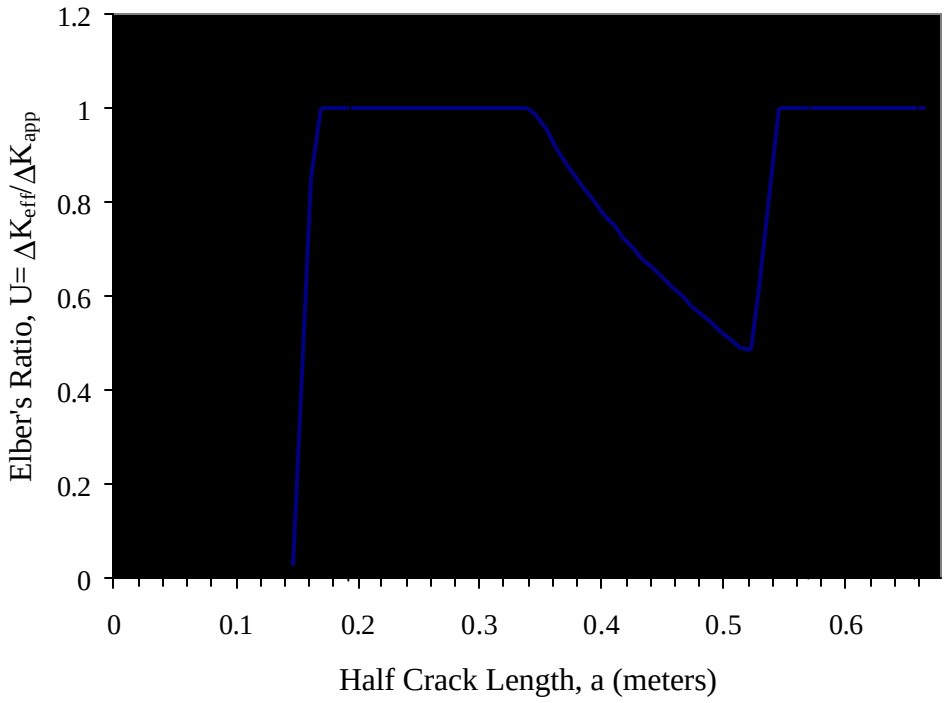

Figure 5-11: Elber's ratio for a stiffened panel with σ_{max}=46 MPa and σ_{min}=6 MPa.

To illustrate this reasoning, suppose one performed an analyses with an initial crack size of a = 0.150 meters and desired a prediction estimate for the crack to reach a = 0.671 meters. The effective stress intensity factors would be very low in the initial crack lengths. As a result, the number of cycles predicted would be very high. On the other hand, if one performed the analysis with an initial crack length with a = 0.165 meters, the initial effective stress intensity factor would be significantly greater. The number of cycles predicted would also be significantly lower, sometimes as small as 10 percent of the previous analysis' estimate. Therefore, it is important to perform the analysis with several starting lengths if the crack originates in a region of compressive stress.

This caution is not as significant in other situations (i.e. running cracks encountering compressive stress) because the applied K continually increases with crack length while the K_r is limited by its self-equilibrium.

5.8 ANALYTICAL PROGRAM

The analytical model may easily be developed in a spreadsheet application. Furthermore, each component may be coded in a separate routine to provide reasonable estimates in a very short amount of time. The analytical model used in this project was developed using Microsoft Excel and accompanying Visual Basic code. The Visual Basic code, which is simply BASIC coding language within the Excel program environment, is integrated into the spreadsheet and may be easily accessed for revisions. A complete program was developed that includes extensive comments for easy interpretation. The routines and flowchart can be found in Appendix B.

The program was developed for the case of a central crack in either an unstiffened plate or stiffened plate. The program does not address a crack emanating from underneath a stiffener or an unsymmetrical crack, but it does provide a solid basis for developing further crack prediction codes.

Other assumptions made include:

1. Equal crack growth rates in the stiffener and the plate. The stiffener is considered severed when the plate crack has propagated a distance equal to the radius of the tangential stiffener distance.

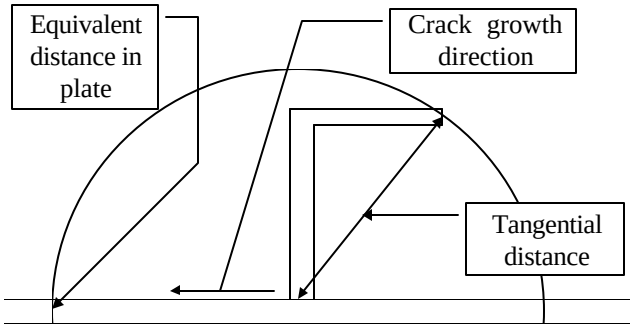

Figure 5-12: Tangential distance for stiffener.

2. Low stress ranges are used and only tensile portion of stress range is considered.
3. Residual stress distribution is unaffected by crack growth.
4. Plasticity affects are negligible or plastic strain reversals provide offsetting results.

Several features have been included in the spreadsheet including a routine that produces Faulkner's residual stress distribution. In addition, instruction is available for each parameter that is required by the program. The end result provides a user-friendly program that was effectively applied in predicting the experimental behavior.

6 Finite Element Model

6.1 INTRODUCTION

The finite element modeling technique is explained in this section. Basically, a finite element analysis is performed on the specified geometry with a given crack length. An output request is made for the J-integral to be calculated, specifying the node at a crack tip and the crack's propagation direction. The J-Integral can then be converted into an equivalent stress intensity factor. Henceforth the procedure is equivalent to that of the analytical model—determining K_{eff} and utilizing it in Equation 2-4 for many discrete crack lengths.

6.2 J-INTEGRAL BACKGROUND

The J-Integral was previously introduced in Chapter 2. It is a measure of the energy released by moving the crack tip forward an incremental length, da. The formal definition is as follows:

$$J = \int_{\Gamma} \left(W dy - T \frac{\partial u}{\partial x} \right) ds = -\frac{\partial V}{\partial a} \qquad \text{Eqn. 6-1}$$

where W is the strain energy density, T is a traction vector (See Figure 6-1) on a point in the contour being evaluated, u is the displacement and s corresponds to the arc length along the contour Γ. The right side of the equation defines the J-integral as the change in potential energy associated with the virtual crack extension, *da*. A graphical aid is shown below in Figure 6-1.

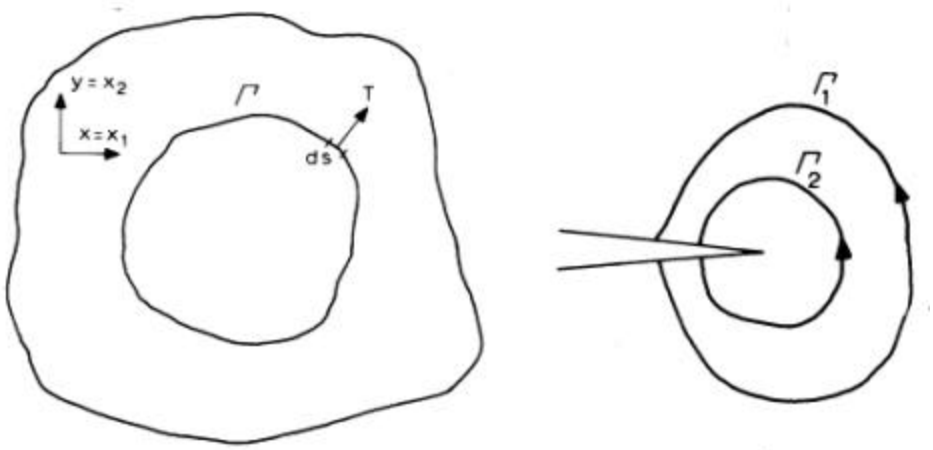

Figure 6-1: Visualization of J-integral evaluation.

The J-integral is calculated using any closed path that encircles the crack tip. A number of separate evaluations may be made along different paths. Each of these evaluations should yield the same value for J since the quantity is path independent in linear elastic materials. In finite element analyses, the first evaluation is usually made using the row of elements immediately surrounding the crack tip. For the modeling put forth in this report, it is suggested that the average of the second and third J-integrals be evaluated. This is because the row of elements immediately adjacent to the crack tip can be subject to stress inaccuracies and therefore yield higher error than subsequent contour paths. J-integral values for paths higher than the third row of elements may also exhibit slight errors in J in regions of high stress gradients.

The path-independent property of the J-integral serves as a check on the accuracy of the J results. It does not, however, assert that the mesh is sufficiently refined to yield the correct stress and displacement values. Therefore, one should perform preliminary mesh studies to find a proper element size. Another useful quality of the path independence is that no special elements are required around the crack tip in most cases. It has been argued in the past that the proper way to model the elastic crack is to include the stress singularity at the crack tip (See Figure 2-4). Barsoum [15] advocated moving the mid-side nodes of six or

eight-noded elements to the ¼ points to correctly recreate the stress singularity. In reality, accurate values for J may be obtained without recreating the stress singularity. Nussbaumer found deviations were 5% on the first contour and less than 1% on the second contour.

The J-integral is only applicable to planar mode I cracks in linear elastic materials [136]. It has been argued that the J-integral may be used for nonlinear material evaluation as well, and the interested reader is referred to the work of [22, 136, 169]. For the proposed fatigue crack growth models, however, one implicitly assumes linear elastic behavior and relatively low stresses. Therefore, the J-integral is well suited for the current research.

Once the J-integral is determined it can be converted into an equivalent K through use of Equation 2-3:

$$K = \sqrt{JE} \quad \text{for plane stress}$$

where E is the material's elastic modulus (MPa), J is in Joules, and K has units of $MPa\sqrt{m}$. The uniqueness of the finite element model ends with the formulation of K, at which point it is used as shown previously in Figure 5-9.

The finite element model was developed using ABAQUS, a powerful finite element software package that was available through the University of Minnesota's Supercomputing Institute. This widely used software is certainly not unique in its capabilities of evaluating the J-Integral, and many F.E. packages exist today with similar features. One such program, ADINA, was used by Nussbaumer to determine stress intensity factors by a method other than the one is this report.

A small plate model will be used in the first section to thoroughly detail the methodology. This case study would be an excellent learning aid for anyone interested in using this method. In Section 6.4, an approach to allow a single set of analyses to be used for various stress ranges is demonstrated. Finally, Section 6.5 details the results of several stiffened panel analyses.

6.3 SMALL MODEL CASE STUDY

The small case study involves modeling a center-cracked tensile (CCT) specimen with residual stresses. Modeling the CCT specimen requires only a quarter of the plate to be modeled (See Figure 6-2).

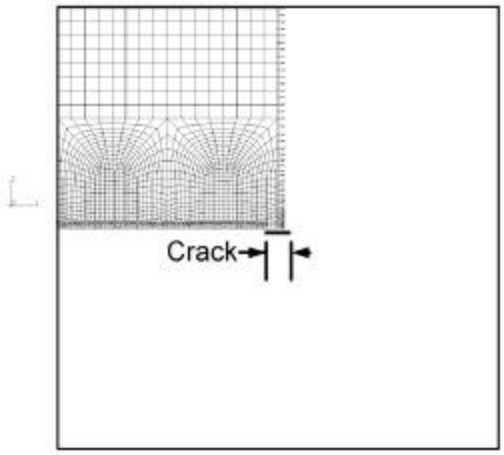

Figure 6-2: Small case study of CCT specimen.

Symmetry conditions are placed along the centerline of the specimen in both the x and y directions. Figure 6-3 shows the mesh and model used, with tensile stress to be applied in the positive y-direction. To simulate a crack, boundary conditions are released along the crack face up to the tip.

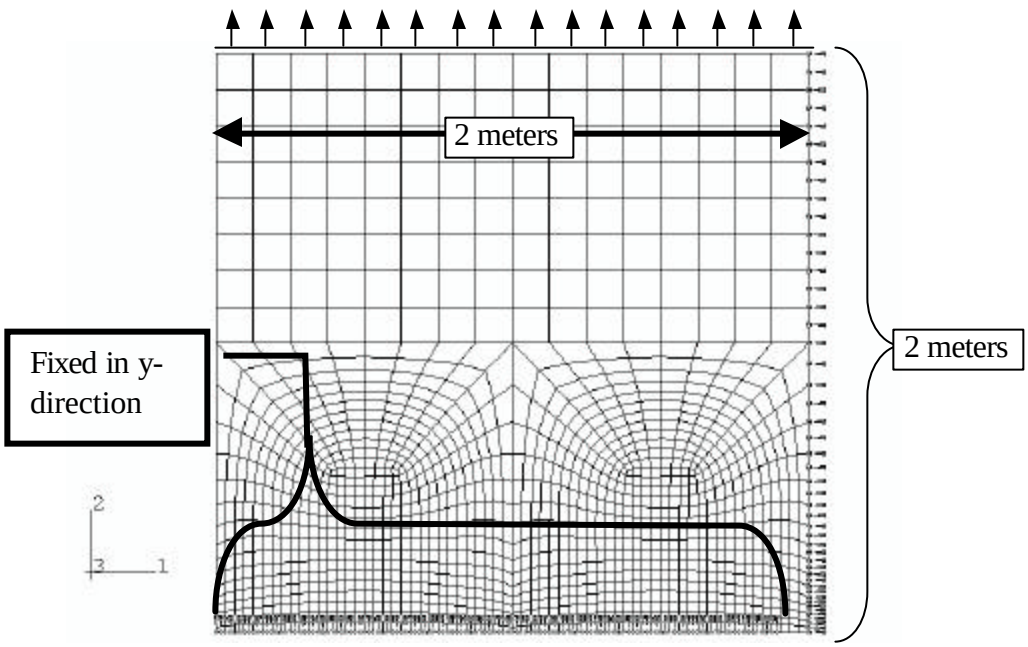

Figure 6-3: Mesh used in small case study.

The mesh is graded so that refined elements are used near the crack plane and coarse elements are used remote from the crack. All elements used in the analyses were 8-noded shell elements with six degrees of freedom at every node. Although all of these degrees of freedom are not required for this plane problem, it is important to have six degrees of freedom in the shells in the three-dimensional stiffened panels because there are 90 degree intersections of shells. Reduced integration was used, which means that there are only four rather than nine integration points. The reduced integration leads to slightly less stiff elements, and typically better displacement results for a given mesh size, although the gradients in the stress within elements are not as well described. These elements were also used in the three-dimensional stiffened panels, however ABAQUS automatically [and appropriately] uses shell elements with full integration at plate intersections. The element size near the crack tip should be roughly the thickness of the plate for reasonable accuracy. This element size may be increased away from the crack tip as long as the geometry of each element is not warped beyond software recommendations. The mesh shown in Figures 6-2 and 6-3 were quickly created using commercial mesh generators, providing a smooth transition between the fine and coarse mesh transition.

Fatigue crack growth requires that many crack lengths be evaluated along the crack line. For this reason it was found convenient to make a zone of refined mesh along the entire crack path. When a new crack length was to be analyzed, no remeshing was required and it was only necessary to release the boundary conditions along the advanced crack face.

Nussbaumer utilized special elements along the crack face to prevent the faces from overlapping in regions of compressive stress. These elements, called "gap elements," yield values for contact forces that occur when two crack faces come together. The resultant contact forces, however, are not included in the J formulation. Therefore, it was decided to examine the effects of using the gap elements in the small CCT study. Case A of the study examines a crack in a tensile residual stress field while Case B examines the same length crack in a region of compressive residual stress. Both cases were subjected to analyses with and without the use of gap elements.

The rest of the finite element procedure is very basic. Forces may be applied as displacements, body forces, temperatures, or nodal forces. A linear static analysis is performed with an output request for the J-integral to be calculated. This request requires the direction cosine of crack propagation to be specified as well as the node number at the crack tip. Applying the forces incrementally allows the computation of the J-Integral at various levels of stress. Typically a load was applied in 10-12 increments over an analyses step. In addition, each type of load (e.g. body forces or temperature) was applied during the analysis as distinct analyses step. Figure 6-4 shows the results of a typical analysis.

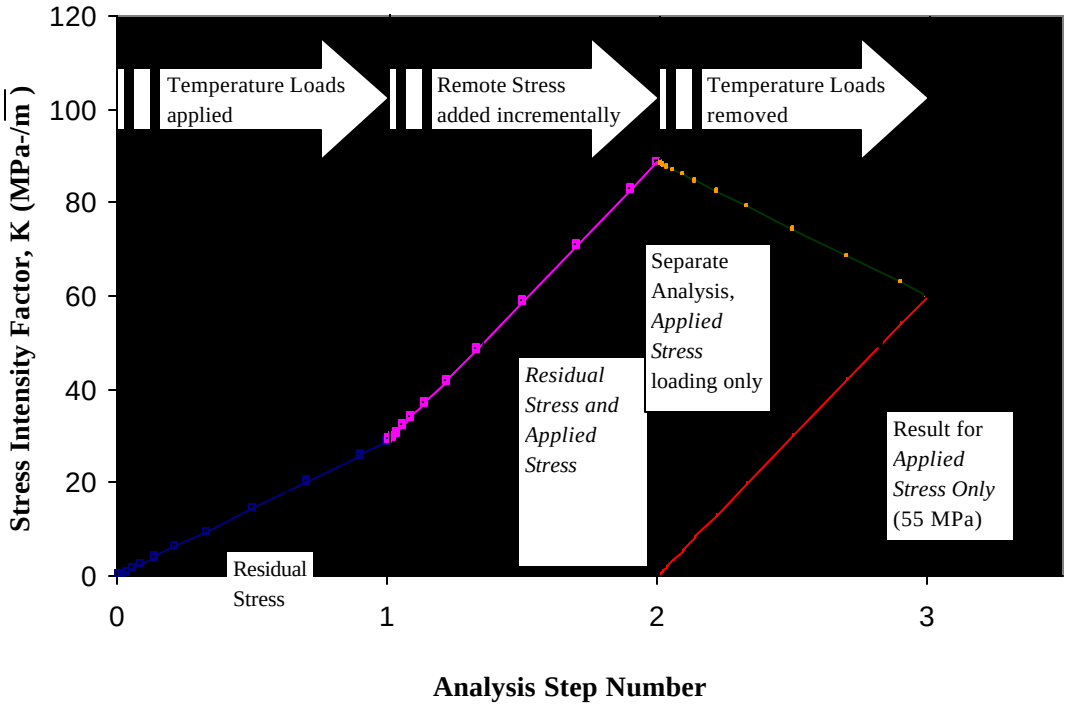

Figure 6-4: Typical plot of analysis procedure.

Residual stresses were modeled by changing the temperature in a region of the specimen. The results of one such analysis, case one, is shown in Figure 6-5. In this figure the temperature of the nodes on the right have been set to –200 Celsius while temperatures on the left have been set to +200 Celsius. The net effect is to create a self-equilibrated bending gradient throughout the specimen, with tensile stresses in the cooled region and compressive stresses in the heated region.

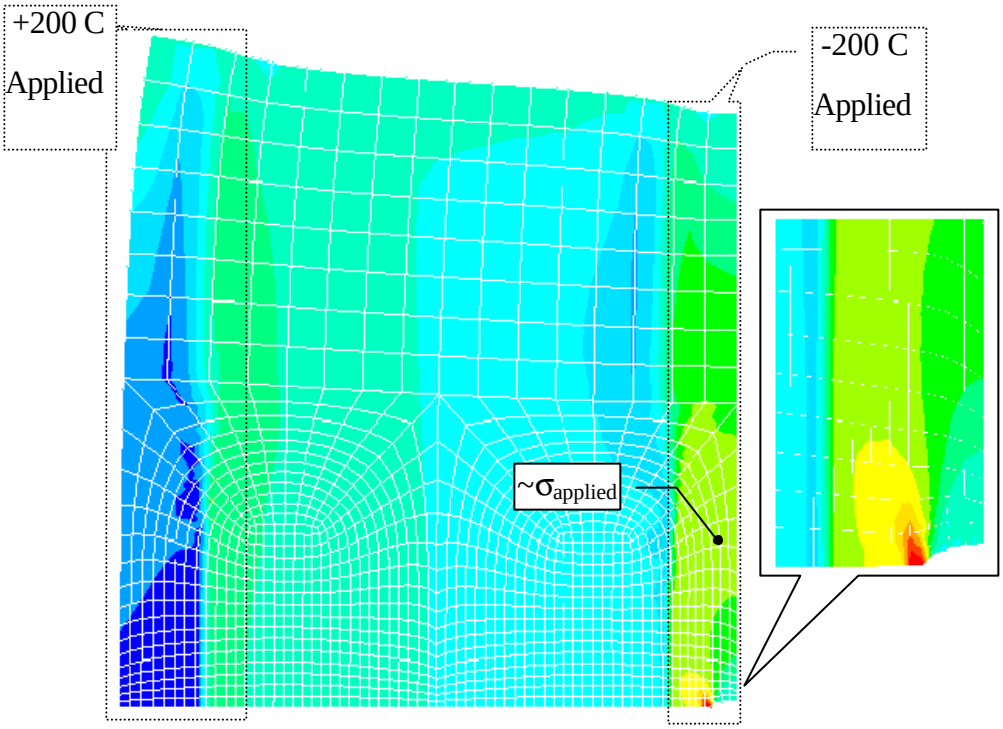

Figure 6-5: Case residual stresses applied by temperature loading.
(100x displacement magnification)

At nodes where the temperature has not been set, the F.E. software applies the default temperature of zero. To roughly verify the computed J-integral, one may take an approximation of the stress above the crack tip and use it in the CCT formula. The computed result should yield a K-value within 35% of the F.E.A. equivalent K value. This crude verification will let the user realize immediately if the approach has been implemented correctly.

An examination of the interaction between residual stress and applied stresses will now be made. Referring to Figure 6-4, one can observe three steps to the analysis. First, the temperature loads are applied and residual stress fields are formed. By performing this step separately, one may directly observe the magnitude of the residual stress J integral. The second step consists of applying forces incrementally without changing the temperature loading. In this CCT study, only body forces were used because they are easily translated

into an applied uniform stress by the analysis. The final step maintains the applied body forces [or other external loading] and incrementally removes the temperature loading. This final step should provide a J estimate equal to that of an applied stress analysis only. To prove this, a separate analysis was performed using the applied body forces only. It is shown plotted with a shift in step number for illustration purposes only.

The use of gap elements makes the analysis more time consuming and difficult. Without their use, however, greater care must be exercised to use the correct J value. To explain, first consider Case A of the study. Its residual stress field has been shown in Figure 6-5. The majority of the crack is subjected to the tensile residual stress field and consequently there are no effects of crack closure. Accordingly, there is no difference between an analysis made using gap elements and that without gap elements. The J integral results for this case are presented in Figure 6-6. A fourth step has been added removing the applied loads to verify the load application cycle.

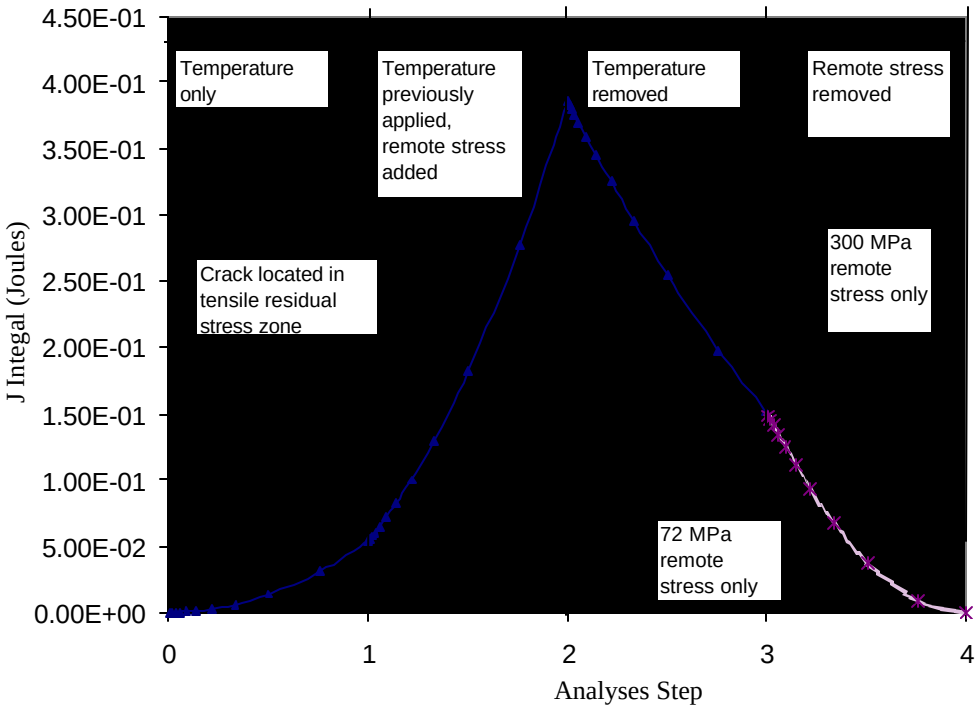

Figure 6-6: Case A of CCT study results.

Notice that the above plot is nonlinear because it plots J instead of K. This point must be kept in mind when using superposition and the Paris Law: A J value must first be converted to an equivalent K before any ΔK is calculated. In other words, do not make the mistake of equating ΔJ with ΔK.

Case B of the CCT study uses the same crack length with reversed temperature loading. Figure 6-7 shows the residual stress distribution from an analysis that did not use gap elements. The overlap caused by compressive residual stress can clearly be seen. With gap elements, no such overlap would occur, effectively maintaining the compressive residual stress at a level equivalent to that of a plate without a crack present.

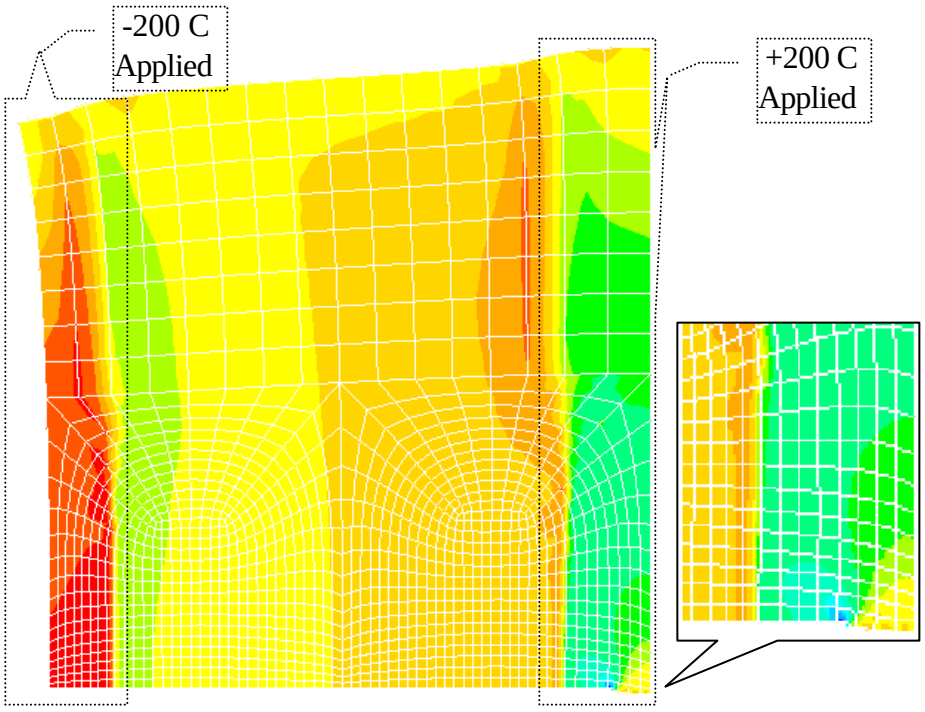

Figure 6-7: Case B residual stresses applied by temperature loading.
(100x displacement magnification)

What's interesting about this study is the behavior of J when gap elements are introduced. The results of Case B are shown in Figure 6-8.

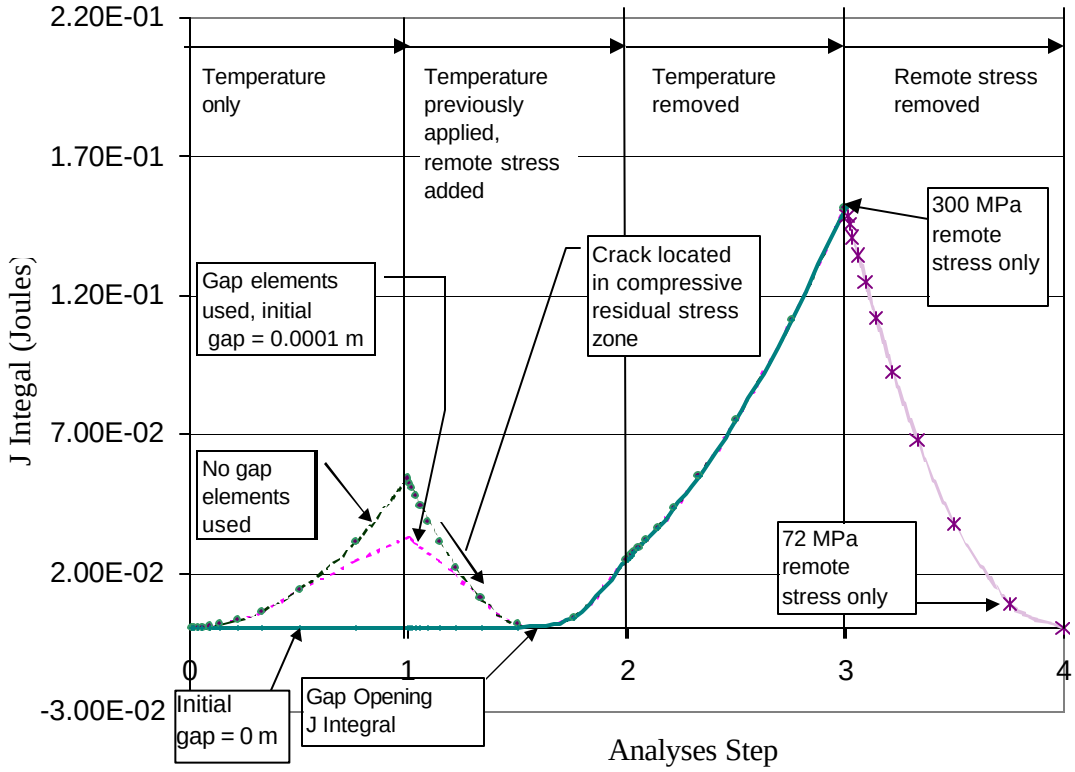

Figure 6-8: Case B of CCT study results.

Some observations can be immediately made from this analysis. First, the J integral is always an absolute value. By omitting gap elements, one is able to observe this characteristic. By including gap elements and specifying an initial gap of zero meters, the J integral remains zero until applied external loads overcome the residual stress-induced closure. By using gap elements with an initial gap of 0.0001 meters, one obtains similar results as would be found without the use of gap elements. This seems to indicate that the J integral may not yield values for the case when there *appears* to be no crack, as in specifying an initial gap of 0 meters.

Without gap elements the J integral is output as an absolute value. A decreasing J with applied tensile load indicates that compressive residual stresses are inducing crack closure. Usually this decrease in J reaches a minimum at the same point as the gap element analysis indicates a non-zero J. The point at which J reaches a minimum under applied loading is the

opening applied load, indicating the applied loads are becoming effective. As the crack tip is moved away from of a region of compressive stress the opening load is decreased. Figure 6-9 demonstrates this for various crack lengths in Case B. At a crack length of 109-mm, the crack is entirely within a region of compressive residual stress. Consequently, the opening load is significantly greater than for a longer crack, especially one that is not completely contained within a compressive residual stress zone.

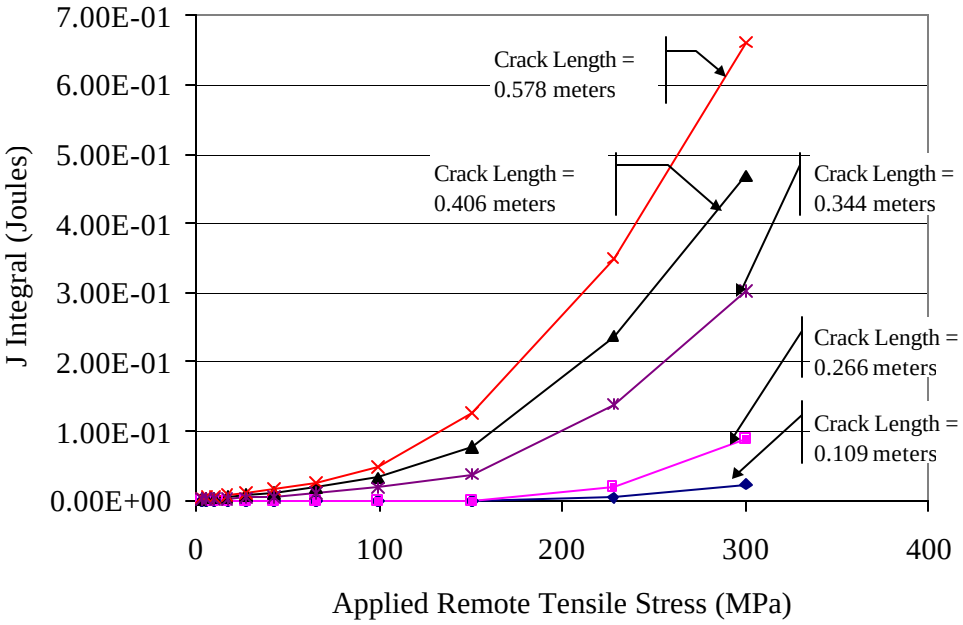

Figure 6-9: Closure effects on effective applied load for Case B.

The three variations of analyzing Case B all converge to a common opening load. This seems to imply the same results could be obtained with or without the use of gap elements. However, the convergence to a common opening load is not always observed. Gap elements take into account closure along the entire crack front, and in some situations the crack may be open near the crack tip while closure occurs behind the crack tip. To illustrate, several variations of closure are illustrated in Figure 6-10 (Adapted from Nussbaumer).

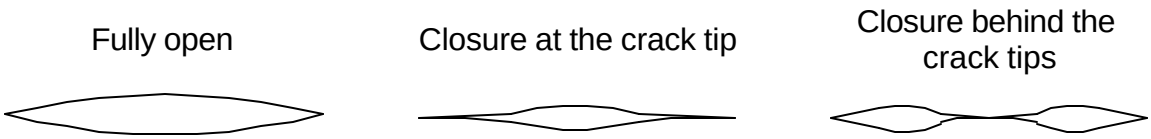

Figure 6-10: Variations of crack shape.

Closure effects behind the crack tip cannot be modeled without the use of gap elements. Proof of this statement was observed in one of the stiffened panel F.E. analyses. In the analysis, a crack was introduced that extended beyond the first severed stiffener. A view of the crack in the panel is seen in Figure 6-11. In this picture, both residual stress and an applied uniform tensile stress of 200 MPa are present.

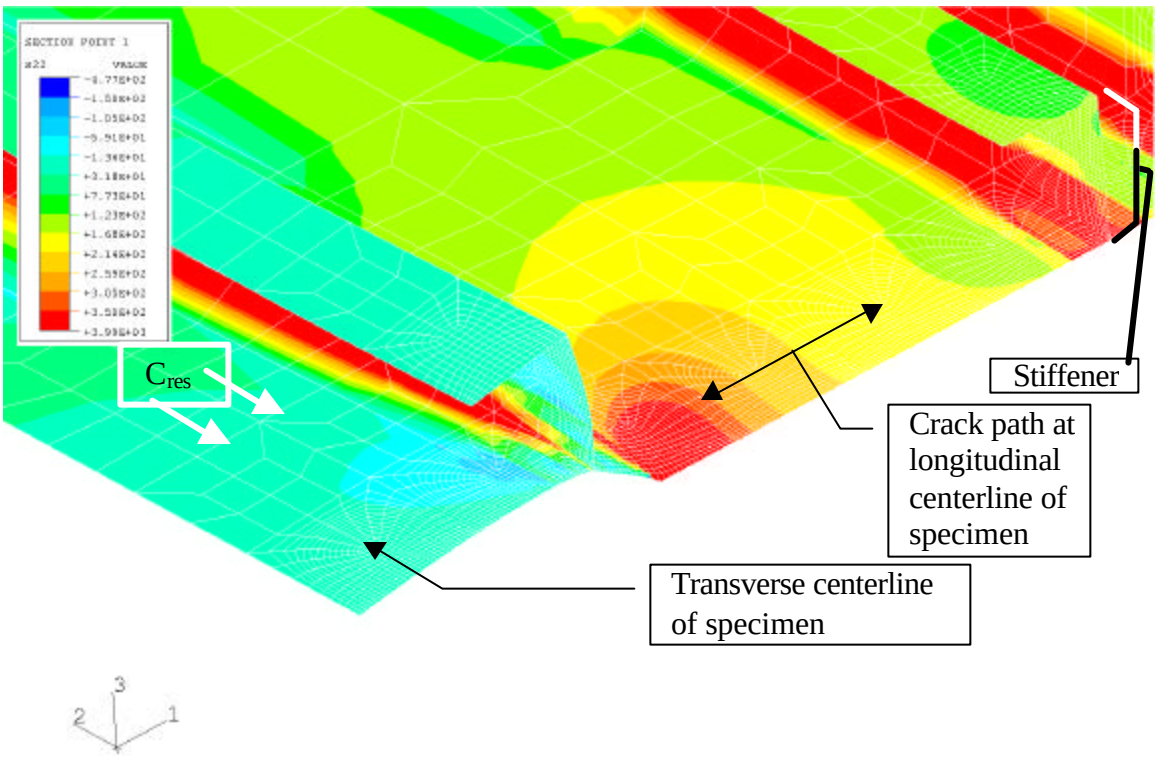

Figure 6-11: Closure effects on effective applied load for Case B.
(100x displacement magnification)

The crack tip was on the outer edge of a tensile residual stress zone, insuring that it would be open even without any applied external load. A region of compressive residual stress exists behind the crack tip. This compressive stress [behind the crack tip] affects the manner in which the crack opens and different results were obtained depending on whether or not gap

elements were used. These differences are quantified in Figure 6-12, where K_{total} is plotted for various phases of load application.

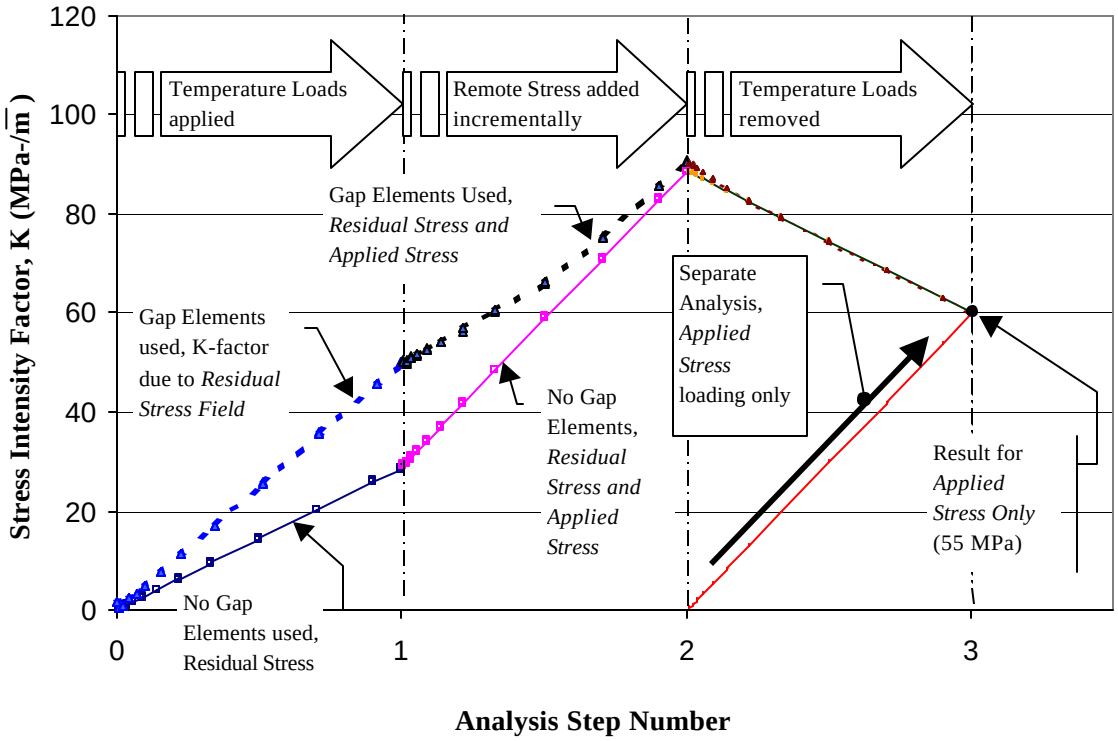

Figure 6-12: Stiffened panel analysis with closure behind crack tips.

Figure 6-12 represents an analysis made with the peak external loading producing 55 MPa of tension in the specimen. Comparing the analysis using gap elements to the one without gap elements provides insight into the merits of each. In the gap element analysis, no overlapping behind the crack tip has occurred and redistribution of residual stress has occurred due to the contact forces. For this reason, the K_{res} derived from a gap element analysis is higher than the analysis where overlapping is permitted. Overlapping, therefore, magnifies closure effects in the analysis without gap elements.

Now consider step two of the analyses. As external load is applied and tensile stresses are induced, the crack starts to open and both analyses converge at a point where closure disappears. The nonlinear behavior of the gap element analysis indicates that residual stress

redistribution is more prominent in the model. In step three, the temperature loading is removed and hence the residual stress field as well. Removing the residual stress field results in no closure effects as pure tension exists in the panel. The fact that removing the residual stress field reduces K_{total} reveals that local tensile residual stress (around the crack tip) was making a significant contribution to K_{total}. A separate analysis has been made without residual stress to show that the same $K_{applied}$ is obtained independently of the three-step analysis method.

One additional observation can be made in reference to Figure 6-12—that of superposition validity. Superposition is only valid in a F.E. analysis made without gap elements. The consequences of nonlinearity will be shown later in comparisons with the analytical model.

Deciding whether or not to use gap elements can now be addressed. The impact of choosing either type of analysis is best illustrated in Figure 6-13. Closure effects that increase the residual stress intensity factor have the effect of decreasing the possible ΔK_{eff}. The Paris Law is a function of the stress intensity factor range, and a smaller available ΔK_{eff} translates into a greater life prediction. While this investigation has isolated the case of closure behind the crack tips, its impact is dramatic on the overall prediction.

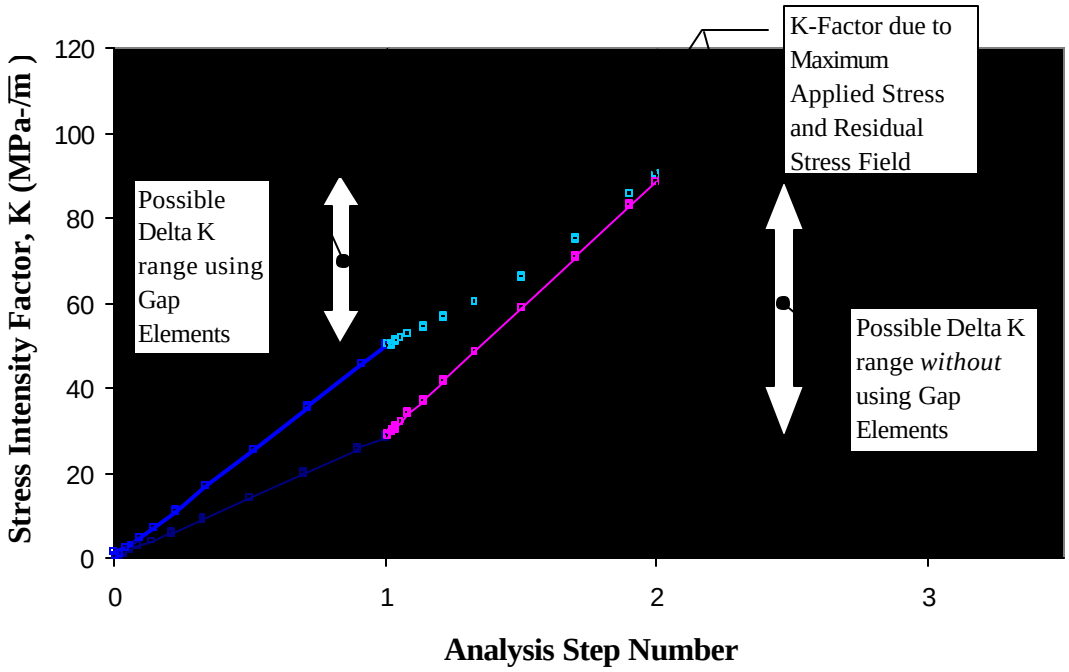

Figure 6-13: Effect of using gap elements in analyses.

Many argue that preventing overlap is the proper way to model cracking in residual stress zones. Specifying an initial gap of zero meters may be called into question. Justification lies in the observation that crack faces are usually jagged and slightly deformed. A perfect meshing of crack faces at the unloaded state is never the case. Instead, contact between crack faces occurs even at initial tensile loading of the structure. Crack tip plasticity after an overload will, of course, prevent contact of crack faces at the unloaded state. Considering the loading history is unrealistic, however, since the analysis already averages all natural variables (e.g. applied stress, material properties, etc.). In addition, it has been emphasized that fatigue crack growth in ship structure often occurs at low stress levels. Such low stress levels advocate low plasticity at the crack tip. For this reason, the initial gap of zero meters is suggested if one intends to model fatigue considering the contact of crack faces.

Is there a correct choice on the use of gap elements? The experimental predictions, presented in Chapter 8, will show better correlation without the use of gap elements. The lack of superposition validity is also a strong argument to not use gap elements in an

analysis that is used for LEFM prediction. In addition, F.E. results obtained from an analysis without gap elements correlate well with the analytical model (See following chapter). Furthermore, the increased complexities of the modeling and increased analysis time make eliminating gap elements favorable. All of these reasons support not using finite element analysis. However, by eliminating gap elements caution must be exercised in making sure the correct opening load (See Figure 6-8) is obtained for all crack lengths. From the current research, it was inconclusive on whether or not gap elements should be utilized. Realistically, contact behind the crack tips should be negligible for cracks greater than one stiffener span. For this reason and because excluding gap elements is conservative, the recommendation is that they are not necessary if proper care is taken in assessing the sign of J (i.e., negative or positive).

There is a convenient way to extrapolate non-gap element results from an analysis that includes gap elements. This method is explained in Figure 6-14. First, an analysis with gap elements is performed with the loads applied in separate steps. This analysis will yield three values for K:

- $K_{res,\ gap}$ (Point 1)
- $K_{total,\ gap} = K_{res,\ gap} + K_{app,\ gap}$ (Point 2)
- K_{app} (Point 3)

The applied stress K, K_{app}, is the same whether or not gap elements are used (Point 3). This fact allows one to merely subtract K_{app} at point three from K_{total} of point 2 to yield the residual stress K that would be obtained from an analysis without gap elements.

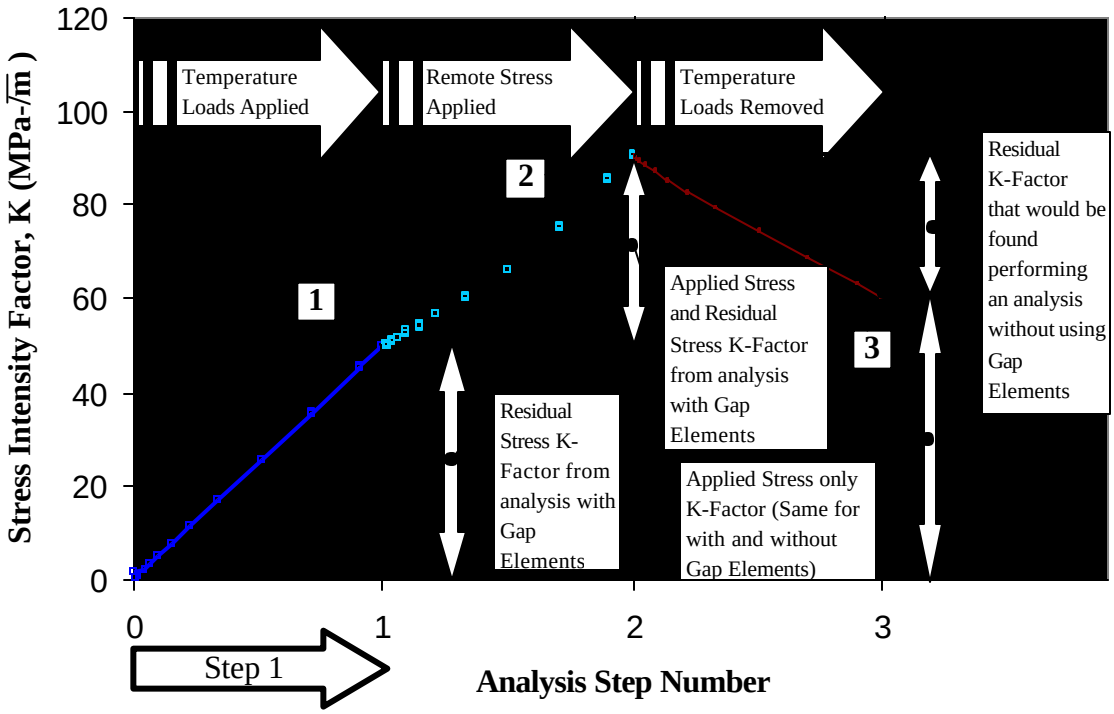

Figure 6-14: Extrapolation of superposition results from a single analysis.

A formal set of expressions clarifies the different obtainable values:

$K_{app,\ gap} = K_{app,\ no\ gap}$ where both values are at point 3

$K_{res,\ no\ gap} = K_{total,\ gap} - K_{app}$ where $K_{total,\ gap}$ is the value at point 2

$K_{res,\ no\ gap} \neq K_{res,\ gap}$ where $K_{res,\ gap}$ is the value at point 1

$K_{res,\ gap} \neq K_{total,\ gap} - K_{app}$

An important requirement for this procedure to work is that all closure effects disappear at peak applied loading. Therefore, one should make the applied stresses large enough to remove any closure effects by the end of step 2.

Applying the loads incrementally has several advantages that will now become evident. Incremental loading allows the history of the J integral to be recorded at discrete values of applied load for a given crack length. The J value for any specific load may be obtained by

first fitting the J history with a natural cubic spline. With little effort, accurate splines were formulated for over 450 step histories of J integrals. One such spline is seen in Figure 6-15. Use of the natural cubic spline has been very successful in comparisons with J integrals determined for the specified load in a separate analysis.

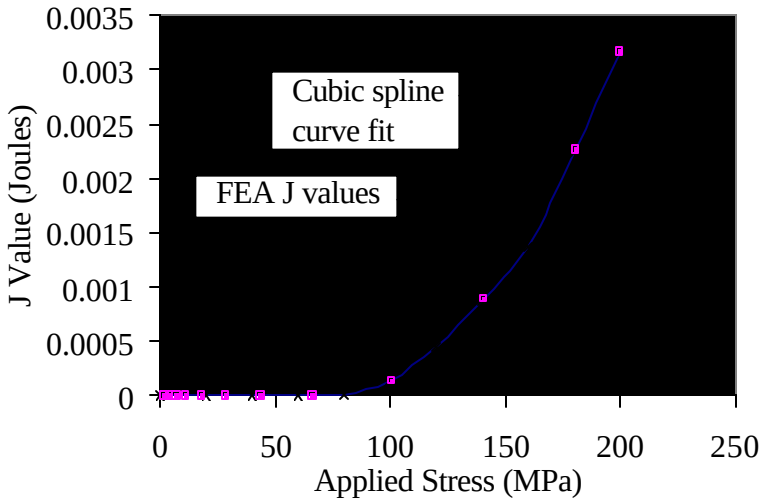

Figure 6-15: Cubic spline fit to incremental J values.

One could also take a simplified yet conservative approach by fitting a linear slope through the equivalent K values as performed by Nussbaumer. This works well for analyses that do not use gap elements because the slopes of K are linear. Either method of extrapolating an equivalent K provides the maximum and minimum values needed to calculate ΔK_{eff}. At this point the Paris Law may be used for prediction.

6.4 STIFFENED PANEL ANALYSES

The finite element model was developed as a tool to model fatigue crack growth in complex geometries. The modeling technique was verified through comparisons with the analytical modeling technique and textbook solutions, such as the CCT specimen in the previous

section. This section will detail the implementation of the model as it was used for formulating equivalent K values in the stiffened panels.

A view of the typical mesh used in these analyses is seen in Figure 6-16. As in the CCT example, symmetry conditions were utilized to model only a quarter of the specimen. Element sizes were typically 12-mm square around the region of the crack line. Smaller element sizes (~5.5-mm) were required to compute converged J estimates in regions of high residual stress gradients. Such high residual stress gradients exist near the transition from compressive to tensile residual stress at stiffener weld lines. In addition, J convergence cannot be obtained close to stiffener/plate intersections. This is because the J integral is a two dimensional quantity.

The crack advancement between analyses should therefore be reduced when the crack is near a stiffener. The trend in J will then reveal any inaccuracies around plate/stiffener junctions.

Crack growth in the stiffeners is a difficult behavior to predict because a crack length must be known as part of the analysis. Therefore, the approach taken was exactly as was done in the analytic model where linear interpolation was used assuming equal crack growth rates in both the stiffener and the plate. Analyses were performed for crack lengths up to the complete plate width for three scenarios: No severed stiffeners, the first stiffener severed, and both stiffeners severed. The broken stiffener analyses were considered only in situations where the crack length was past the stiffener in question. The behavior was usually similar to the plot in Figure 6-17.

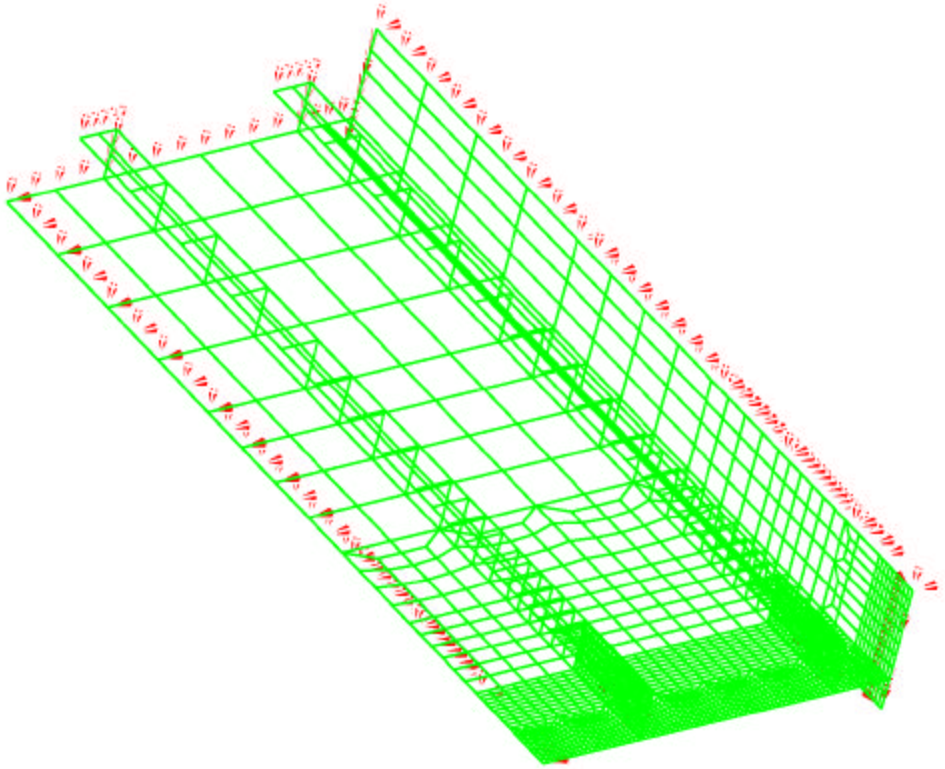

Figure 6-16: Typical mesh of stiffened panel.

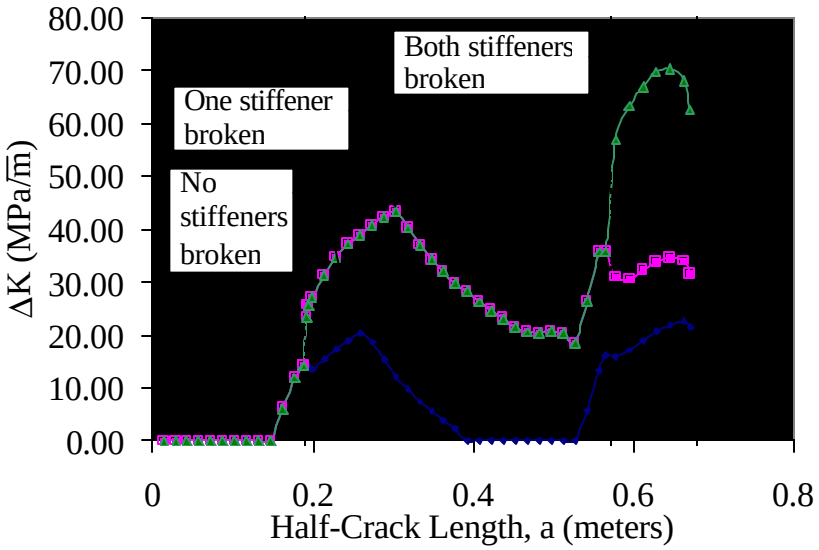

Figure 6-17: K_{total} for typical analysis of stiffened plate.

To create accurate residual stress fields, temperature gradients were applied to nodes near the weld line (See Figure 6-18). A thermal expansion coefficient of 1.2 x 10^{-5}/ degree Celsius and an initial temperature of 25 degrees Celsius were used in defining the material properties. Iteration was required to find the appropriate temperature values, but it was found that cooling the material to a temperature (in Celsius) roughly equal to two-thirds the stress desired (MPa) produced an appropriate distribution. An upper bound residual stress field was obtained by applying the following temperature profile to the nodes within 3.5 times the plate thickness from a weld line.

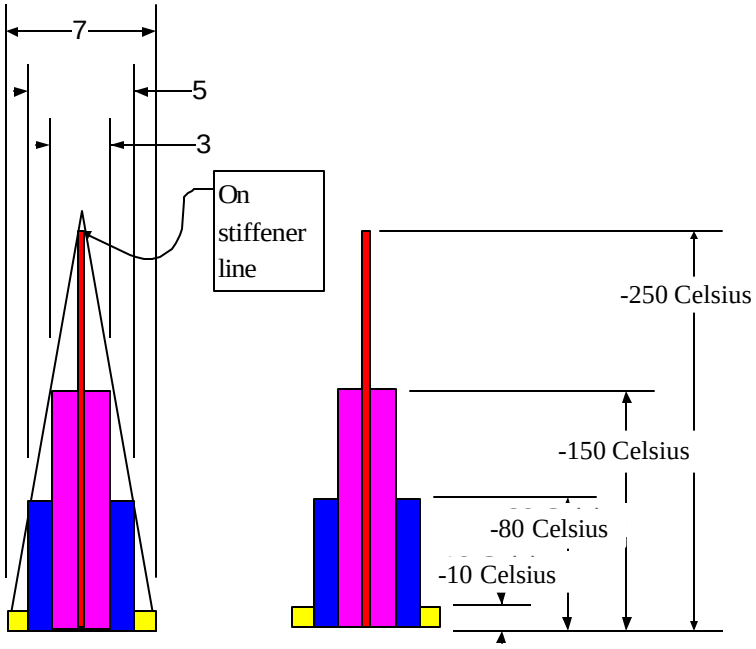

Figure 6-18: Temperature distribution applied to weld lines.

All nodes within a distance specified by the drawing on the left were applied the corresponding temperatures on the right drawing. The distances given are multipliers of the plate thickness. By using this methodology a good approximation to welding residual stresses can be created.

Compressive residual stresses were essentially constant at a value of –70 MPa between tensile regions. Tensile stresses along weld lines sometimes exceeded the yield strength of the material by 40 MPa, but this discrepancy was deemed acceptable. A view of the residual stresses imparted on a typical specimen may be seen in Figure 6-19.

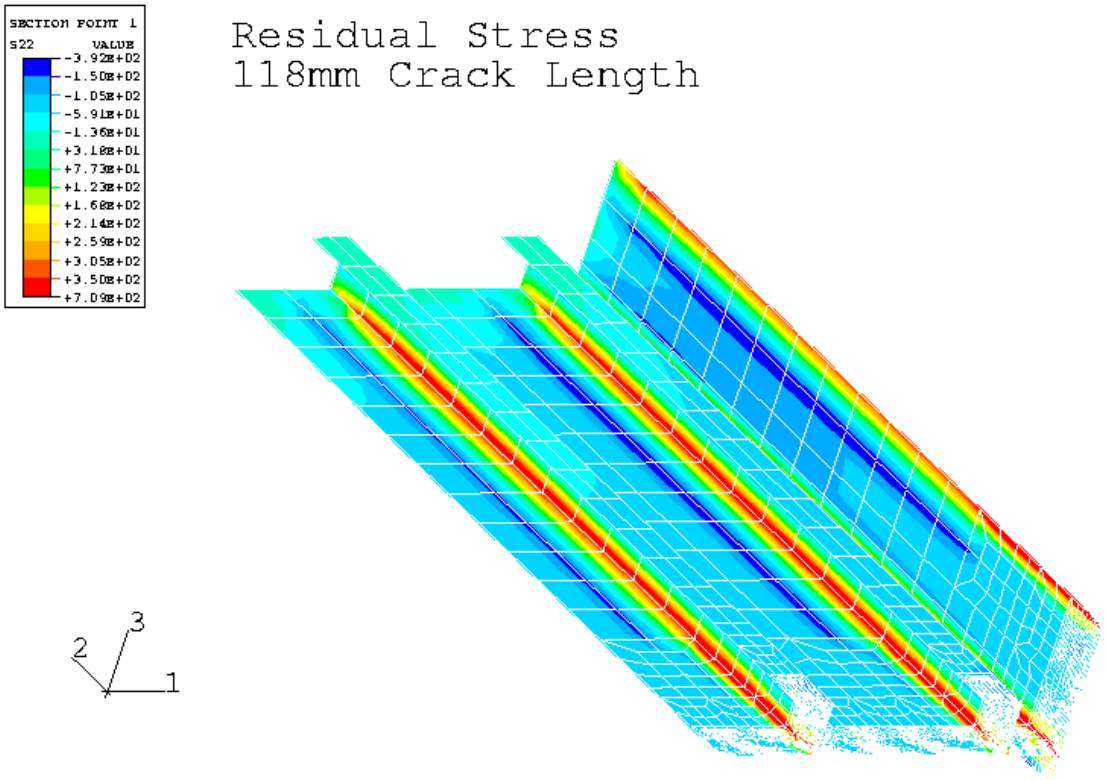

Figure 6-19: Typical residual stress distribution created in specimens.

Comparisons were made between applied displacements and applied stresses. As expected, equivalent K values were progressively less than those of the applied stress analyses. The stagger is especially noticeable when stiffeners are severed as may be seen in Figure 6-20. Here the equivalent K values have been normalized by the CCT K equivalent for the crack length. Also, the crack distance has been normalized by the stiffener spacing.

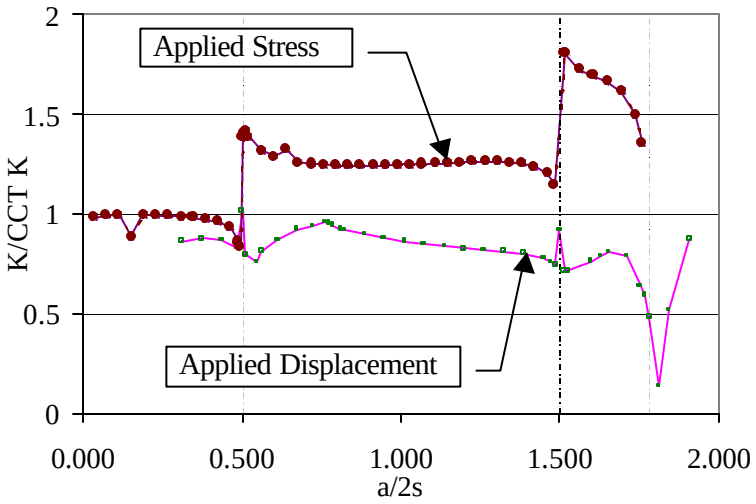

Figure 6-20: Applied stress versus displacement results in Case 1.

Note that several data points seem slightly out of place with respect to the trend lines. Inconsistent J values will be found at times even with mesh refinement. It is therefore important to combine a number of crack length analyses with plotting, such as the above figure, to recognize any erroneous data points.